HHS Public Access

Author manuscript

Exp Eye Res. Author manuscript; available in PMC 2020 May 01.

Published in final edited form as:

Exp Eye Res. 2019 May ; 182: 74–84. doi:10.1016/j.exer.2019.03.011.

Cannabinoid CB2R receptors are upregulated with corneal injury and regulate the course of corneal wound healing

Natalia Murataeva[1], **Sally Miller**[1], **Amey Dhopeshwarkar**[1], **Emma Leishman**[1], **Laura Daily**[1], **Xavier Taylor**[1], **Brian Morton**[1], **Matthew Lashmet**[1], **Heather Bradshaw**[1], **Cecilia J. Hillard**[2], **Julian Romero**[3], and **Alex Straiker**[1]

[1]The Gill Center for Biomolecular Science and the Department of Psychological and Brain Sciences, Indiana University, Bloomington, IN 47405, USA.

[2]Department of Pharmacology and Toxicology, Neuroscience Research Center, Medical College of Wisconsin, Milwaukee, WI, USA.

[3]Faculty of Experimental Sciences, Universidad Francisco de Vitoria, Pozuelo de Alarcón, 28223, Madrid, Spain

Abstract

CB2R receptors have demonstrated beneficial effects in wound healing in several models. We therefore investigated a potential role of CB2R receptors in corneal wound healing. We examined the functional contribution of CB2R receptors to the course of wound closure in an *in vivo* murine model. We additionally examined corneal expression of CB2R receptors in mouse and the consequences of their activation on cellular signaling, migration and proliferation in cultured bovine corneal epithelial cells (CECs). Using a novel mouse model, we provide evidence that corneal injury increases CB2R receptor expression in cornea. The CB2R agonist JWH133 induces chemorepulsion in cultured bovine CECs but does not alter CEC proliferation. The signaling profile of CB2R activation is activating MAPK and increasing cAMP accumulation, the latter perhaps due to G_s-coupling. Lipidomic analysis in bovine cornea shows a rise in acylethanolamines including the endocannabinoid anandamide 1 hour after injury. In vivo, CB2R deletion and pharmacological block result in a delayed course of wound closure. In summary, we find evidence that CB2R receptor promoter activity is increased by corneal injury and that these receptors are required for the normal course of wound closure, possibly via chemorepulsion.

Keywords

cornea; corneal wound healing; lag phase; cannabinoid; endocannabinoid; CB2; chemotaxis

Corresponding author: Alex Straiker, 1101 E 10th St, Bloomington, IN 47405, Tel: (206) 850 2400, straiker@indiana.edu.

1 INTRODUCTION

Cannabinoid receptors were once chiefly known as the endogenous target for the psychoactive ingredients of marijuana (Gaoni and Mechoulam, 1964). However, it is now appreciated that the endogenous cannabinoid signaling system is important in its own right, playing physiological roles in pain, neurodegeneration, appetite and energy regulation, learning and memory, addiction, bone homeostasis and remodeling, cancer, immune function, cardiovascular function, and reproduction (Howlett et al., 2004; Kano et al., 2009). Cannabinoids are also active in the eye, where CB1R receptors are widely expressed (Straiker et al., 1999a; Straiker et al., 1999b). CB1R activation alters intraocular pressure, iridial contraction and perhaps vision (reviewed in (Cairns et al., 2015)). Deleterious mutations of the endocannabinoid-metabolizing enzyme ABHD12 in humans result in the development of cataracts and retinal degeneration (Fiskerstrand et al., 2010). CB1R receptors are abundant in human corneal epithelial cells (CECs) (Straiker et al., 1999b) and mediate chemotaxis in cultured bovine CECs (Murataeva et al., 2016). Importantly, CB1R deletion slows wound healing (Yang et al., 2013), suggesting that cannabinoids, via CB1R, regulate the rate of wound closure via a chemotaxic mechanism, using an endocannabinoid gradient to provide directional cues to CECs during the healing process (Murataeva et al., 2015).

CB2R receptors were identified shortly after CB1R (Munro et al., 1993) but the data on ocular CB2R has been mixed: most receptor expression studies have not detected CB2R in the anterior eye (Buckley et al., 1998; Lu et al., 2000; Porcella et al., 1998; Porcella et al., 2000), but a few pharmacological studies provide evidence for functional CB2R in the eye (He and Song, 2007; Zhong et al., 2005). Cannabinoid pharmacology can however be problematic; we have shown for instance that CB2R agonist JWH015 (used in (He and Song, 2007; Zhong et al., 2005)) is also a potent and efficacious CB1R agonist (Murataeva et al., 2012).

CB2R receptors have demonstrated beneficial effects in wound healing in several models (Li et al., 2016; Wang et al., 2016; Wright et al., 2005; Zheng et al., 2012) and been shown to regulate chemotaxis in immune-related cells such as lymphocytes (e.g. (Ghosh et al., 2006)). The current study investigates CB2R upregulation upon corneal injury and its role in corneal wound healing.

2 MATERIAL AND METHODS

2.1 Animals

Experiments were conducted at the Indiana University campus. All mice used for experiments were handled according to the guidelines of the Indiana University animal care committee and in accordance with the ARVO animal statement. Mice (age 3–8 months) were kept on a 12 h (06:00–18:00) light dark cycle, and fed *ad libitum*. Male and female C57BL/6J (C57) and CD1 strain mice were kindly provided by Dr. Ken Mackie (Indiana University, Bloomington IN). Mice were allowed to acclimatize to the animal care facility for at least a week prior to their use in experiments. CB1R KO and CB2R KO mice were kindly provided by Dr. Ken Mackie. The KOs are all global KOs. CB1R KO animals were

originally received from Dr. Catherine Ledent (Catholic University, Leuven) as heterozygotes (Ledent et al., 1999). The CB2R KO mice were originally purchased from Jackson Labs (Bar Harbor, ME).

2.2 Generation of CB2R-GFP Reporter Mice

Generation of CB2R-GFP reporter mice has been described (Lopez et al., 2018, In Press). Briefly an eGFP reporter gene preceded by an IRES sequence was inserted into the 3' UTR of the *cnr2*, (CB2R) gene into the embryonic stem cells of C57BL/6j mice. This resulted in the expression of floxed eGFP under the control of the endogenous mouse CB2R promoter. The mouse model (CB2R eGFP/f/f) was generated by homologous recombination in embryonic stem cells, in the C57BL/6J genetic background.

2.3 Bovine Corneal Epithelial Cell culture

Bovine CECs (bCECs) were harvested from cow eyes obtained from healthy animals of the species *Bos primigenius taurus* at a local farm. bCECs were dissociated with a combination of trypsin (0.25%) treatment and scraping. Cells were then grown in SHEM media containing DMEM (44%), F-12 (44%), fetal bovine serum (10%), penicillin/streptomycin (1%), amphotericin (2.5 μg/mL), insulin (5 μg/mL), EGF (5 ng/mL). Note that in contrast to our previous study (Murataeva et al., 2015) we avoided the use of DMSO in this SHEM media. Cells received a media change every third day and were subcultured once the flask reached 75% confluence. Cells were not cultured past the third passage.

2.4 Immunohistochemistry

For immunohistochemistry, mouse eyes were fixed in 4% paraformaldehyde for 45 mins at 4 °C, then placed sequentially in 10% and 30% sucrose in PBS overnight before being quick-frozen in OCT. Fixed eyes were sectioned on a Leica cryostat, then sections were mounted on Superfrost plus slides. Slides were blocked with BSA, followed by treatment with primary antibodies (in PBS, saponin, 0.2%) for 1–2 days at 4°C. In cases where secondary antibodies were required, a second staining with secondary antibody (~4 hrs at RT) was done after washing off the primary antibody. Primary antibodies were Anti-GFP (Prelabeled with Alexa647; Thermo Scientific, A-31852), phalloidin preconjugated to Alexa488 (Thermo Scientific, cat#: A12379), and Laminin-5 (AB14509, Abcam) followed by Alexa647 anti-rabbit (A-150075, Thermo Scientific). Slides were then mounted (Fluoromount, Sigma-Aldrich, St. Louis, MO) and coverslipped to prepare for imaging. Images were acquired with a Leica TCS SP5 confocal microscope (Leica Microsystems, Wetzlar, Germany) using Leica LAS AF software and a 63X oil objective. Images were processed using ImageJ (available at http://rsbweb.nih.gov/ij/) and/or Photoshop (Adobe Inc., San Jose, CA). Images were modified only in terms of brightness and contrast.

2.5 Cell proliferation assay

bCECs were plated at a concentration of 10000 cells/well in a 96 well plate in serum-free SHEM medium. After 30 hours incubation under various treatment conditions, the cells were labeled with nuclear marker DRAQ5, the slides were imaged on an Odyssey scanner (LiCOR Biosciences, Lincoln, NE).

2.6 Signaling assays

Cyclase assays: Cyclase assays were optimized using Perkin Elmer's LANCE® Ultra cAMP kit (Catalog # TRF0262, Perkin Elmer, Boston, MA) following the manufacturer's instruction. All assays were performed at room temperature using 384-optiplates (Catalog# 6007299, Perkin Elmer). Briefly, cells were resuspended in 1X stimulation buffer (1X Hank's Balanced Salt Solution (HBSS), 5 mM HEPES, 0.5 mM IBMX, 0.1% BSA, pH 7.4, made fresh on the day of experiment). Cells (10 μL/well; 5000 cells/well) were incubated for 1 hour at 37° C, 5% CO_2 and humidified air and then transferred to a 384-optiplate (500 cells/μl, 10μl), followed by stimulation with drugs/compounds made in 1X stimulation buffer as appropriate, for 10 mins. Cells were then lysed by addition of 10μl Eu-cAMP tracer working solution (4X, made fresh in 1X lysis buffer supplied with the kit; under subdued light conditions) and 10μl Ulight™ anticAMP working solution (4X, made fresh in 1X lysis buffer) and further incubated for 1 hour at room temperature. Plates were then read with the TR FRET mode on an Enspire plate reader (Perkin Elmer, Boston, MA).

MAPK assay: Cells were plated at 75000 cells/well on poly-D-lysine coated 96 well plates overnight in serum-free conditions (37° C, 5% CO_2, humidified air). The following day, cells were challenged with compounds made in serum-free media for 5 mins. Cells were fixed in 4% PFA for 30 mins followed by further 15 min incubation with methanol at −20° C. Plates were washed with TBS/0.1% Triton X-100 for 25 mins (5 × 5 min washes). The wash solution was then replaced by Odyssey blocking buffer and incubated further for 90 min with gentle shaking at room temperature. Blocking solution was removed and replaced with blocking solution containing anti-phospho-$ERK_{½}$ antibody (1:150; Cell Signaling Technology®, Danvers, MA); antibody exposure occurred overnight with shaking at 4°C. The next day, plates were washed with TBS containing 0.05% Tween-20 for 25 min (5 × 5 min washes). Secondary antibody, donkey anti-rabbit conjugated with IR800 dye (Rockland, Limerick, PA), prepared in blocking solution, was added and gently shaken for 1 hour at room temperature. The plates were then again washed 5 times with TBS/0.05% Tween-20 solution. The plates were patted dry and scanned using LI-COR Odyssey scanner. $pERK_{½}$ activation (expressed in %) was calculated by dividing average integrated intensities of the drug treated wells by average integrated intensities of vehicle-treated wells. All assays were performed in triplicate, unless otherwise stated.

2.7 Live-imaging migration assay

In vitro cell migration was also visualized using an upright Nikon E800 microscope fitted with a Hamamatsu Orca-ER camera and Metamorph acquisition software. The microscope was housed in an environmental chamber that regulated temperature (33° C), and pH by streaming humidified carbogen over the samples. This whole apparatus was covered in a grounded Faraday cage. Images were acquired using a 4x objective over the course of an hour at 10-second intervals. Cells were tracked using the mTrackJ software plugin (Meijering et al., 2012) for ImageJ (http://www.imagescience.org/meijering/software/mtrackj/). JWH133 was embedded in 1.5% agar prepared from serum-free media on the day of the experiment. Cells were maintained in serum-free media overnight before plating into 60mm petri dishes coated with poly-D-lysine. Movement of cells within the dish was monitored before and after placement of a cube (<1 cm^3) of drug- embedded agar at the

edge of the dish. The location of the agar cube was varied to address the possibility of migration due to other environmental factors such as electric fields. The concentration of JWH133 was chosen based on our Boyden Chamber-derived concentration-responses for WIN55212 and 2-AG (Murataeva et al., 2015).

2.8 In vivo corneal wound healing study.

A ~ 1 mm diameter circular axial corneal epithelial defect was created in an isoflurane-anesthetized mouse using an Alger Brush under a stereomicroscope. We used mechanical debridement, a method similar to that used by Yang et al. (Yang et al., 2013), but with distinctions regarding the size of the wound and the interval of monitoring the healing process. When drugs (JWH133, SR144528) were applied, these were dissolved in Tocrisolve then applied as 5uL drops to the eyes of C57 mice after injury but while animal was still anesthetized. The mouse was briefly re-anesthetized with isoflurane at 3 hour intervals to monitor the progress of corneal wound healing. Wound area was measured by staining the eye with fluorescein (0.2 mg/mL in PBS) and was illuminated with a blue-violet light source and photographed using a camera-mounted stereomicroscope. Wound area was quantified using ImageJ. The basement membrane is intact after wounding as demonstrated by Laminin-5 staining (Supplementary Figure 1).

2.9 Quantitative RT-PCR

Primers for selected components of the endocannabinoid system were designed using Primer-Blast (http://www.ncbi.nlm.nih.gov/tools/primer-blast) and the corresponding mouse gene. Primer sequences are as listed,

msCB1R S: 5′ - CTG ATC CTG GTG GTG TTG ATC ATC TG 3′

msCB1R AS: 5′ - CGT GTC TGT GGA CAC AGA CAT GGT 3′

msCB2R S: 5′ - AAA GCA AGG AGG TCC ACT CG 3′

msCB2R AS: 5′ - GCC GTT GAC CTT CAC AGA GA 3′

msGPR18-S 5′- CAG CCT TTG ACA GAC AGG AGG TTC -3′

msGPR18-AS 5′- AGC CAC AGA GCG AGG CTT GG -3′

msGPR119-S 5′- CTT CTT CTA CTG TGA CAT GCT CAA GAT TGC -3′

msGPR119 -AS 5′- GCC AAT AGG CAT AGA TGA GTG GGT TG -3′

msNAPE-PLD-S 5′- GCA GCT GGT CCG TGC TAG GG -3′

msNAPE-PLD-AS 5′- CTG GCG GCT CTA GGT AAT GCT CA -3′

msFAAH-S 5′- CAA ACA GAA ACA GCC CCT GC -3′

msFAAH-AS 5′- TCC CTC CCT TCA CTT GTC CT -3′

Eyes were extracted, the lens removed, and were then immediately stored at −80°C. RNA was extracted using a Trizol reagent (Ambion, Austin, TX) and genomic DNA was removed with DNase (NEB, Bethesda, MD) following the manufacturer's instructions. RT-PCR was performed using a one-step, Sybr Green amplification process (PwrSybr, Applied

Biosystems, Carlsbad, CA). Quantitative PCR was performed using an Eppendorf RealPlex2 Mastercycler thermocycler.

GAPDH mRNA expression was used as an internal control for each experimental condition with the threshold cycle set within the linear range (10 fold above baseline). Once the standard critical threshold (Ct) was set, the relative expression levels for genes were determined. Data analysis and statistics were performed using Excel (Microsoft Corp., Redmond, WA) and Prism (GraphPad Software Inc., San Diego, CA) software. Values were compared using an unpaired t-test.

2.10 Lipidomic analysis of bovine corneal injury

The lipidomic consequences of injury were tested in the eye of the cow. The cow eye is far larger than the mouse eye and so better suited to reliable quantification of lipidomic changes. Moreover, post-mortem injury allows the separation of cornea-specific responses to injury. Cow eyes were obtained as above. Corneas were removed and injured by scratching then maintained in saline. Injured and non-injured controls were then prepared for lipidomic analysis.

Corneas were flash frozen in liquid nitrogen and frozen at −80°C until used for lipid analysis. Levels of ~35 cannabinoid-related lipids as well as arachidonic acid and several prostaglandin-family metabolites were measured by liquid chromatography/mass spectrometry from whole eyes as previously described (Bradshaw et al., 2009; Miller et al., 2017). Briefly, corneas were homogenized, centrifuged at 19,000 × g at 24°C for 20 min and supernatant was collected. Compounds were isolated using a partial purification of the 25% organic solution. C18 solid-phase extraction columns (Agilent Technologies, Santa Clara, CA) were used with an elution of 100% methanol.

Samples were placed in an autosampler and held at 24°C (Agilent 1100 series autosampler, Palo Alto, CA) for LC/MS/MS analysis. 10–20 μL of eluents were injected for each sample that was rapidly separated using a C18 Zorbax reversed-phase analytical column (Agilent Technologies, Santa Clara, CA) to scan for individual compounds. Gradient elution (200 μL/min) then was accomplished under pressure (Shimadzu 10AdVP pumps, Columbia, MD). The electrospray ionization was done using an API3000 triple quadrupole mass spectrometer (Applied Biosystems/DSM Sciex, Foster City, CA). A multiple reaction monitoring (MRM) setting on the LC/MS/MS was used to analyze levels of each compound. Analysis of the HPLC/MS/MS data was performed using Analyst software (Applied Biosystems Sciex). Chromatograms were generated by determining the retention time of analytes with a [M-1] or [M+1] parent peak and a fragmentation peak corresponding to the programmed values. The retention time was then compared with the retention time of a standard for the suspected compound. If the retention times matched, then the concentration of the compound was determined by calculating the area under the curve for the unknown and comparing it with the calibration curve obtained from the corresponding standards. Extraction efficiency was calculated relative to the standard-spiked recovery vial. Concentrations in moles per gram adjusted for percent recovery from the experimental condition with the untreated condition using a 1-way ANOVA. All statistical tests were carried out using SPSS Statistics 20 (IBM,

Armonk, NY, USA). Statistical significance was defined as $P \leq 0.05$ and a trending effect was defined as $0.05 < P \leq 0.10$.

2.11 Drugs

JWH133 was purchased from Tocris Biosciences (Bristol, UK). SR144528 was purchased from Sigma-Aldrich (St. Louis, MO). Epithelial growth factor (EGF) was purchased from Invitrogen (Carlsbad, CA)

3 RESULTS

3.1 CB2R ligands induce chemorepulsion in cultured bovine corneal epithelial cells.

The CB2R agonist JWH133 (300nM) was embedded in a cube of agar and placed in a 60mm petri dish containing recently plated bCECs. As depicted schematically in Fig 1A, the JWH133-containing agar block was positioned at the edge of the dish while the migration of epithelial cells at the center of the dish was monitored. The sample migration tracks from one experiment are shown in Figure 1B. Migration of cells was arrested after subsequent bath application (i.e. no gradient) of CB2 antagonist SR144528 (250nM, Fig. 1B, inset). We found that in contrast to the previously CB1 activation that induces chemoattraction (Murataeva et al., 2015), the CB2R agonist JWH133 induced *chemorepulsion* in bCECs (Fig. 1C–D; baseline velocity away from target (μm/min ± SEM): 0.33 ± 0.69; JWH133 (300nM in agar): 5.10 ± 0.99; the addition of CB2R antagonist SR144528 (SR2, 250nM) to the bath inhibited the effects of JWH133 on migration JWH133 + SR2 (250nM bath): 1.25 ± 0.44; n=18; significant effect of JWH133 on migration using 1 way ANOVA and Bonferroni post-hoc test [$F(3,17) = 11.8$, $p = 0.0003$].

3.2 CB2R activation paradoxically activates both pERK and cAMP signaling

As a $G_{i/o}$-coupled receptor, CB2R would be expected to activate the MAPK pathway and inhibit adenylyl cyclase activity. The CB2R agonist JWH133 increased MAPK activity measured as ERK phosphorylation (Figure 2A; EC_{50} (95% CI): 78 nM (87.4–111.2); E_{max} (± SEM): 46 ± 5.6), but also modestly increased adenylyl cyclase activity even in the presence of forskolin (Figure 2B; EC50 6.2 nM (1.1–23.6); Emax: 36 ± 7.3). In both cases, the effect was blocked by including the CB2R antagonist SR144528 (SR2, 1μM; $p<0.01$, Student's t test for 1μM SR2 vs. 1μM JWH133). We repeated the experiment without forskolin, since forskolin would presumably be occluding CB2R activation, and found that without forskolin the CB2R agonist JWH133 resulted in greater activation of adenylyl cyclase (Figure 2C: EC_{50}: 7.2 nM (0.5– 17.6); E_{max}: 48.2 ± 6.5). The antagonist SR2 had no effect on its own in the pERK assay, but lowered cAMP accumulation in the absence of forskolin ($p<0.01$, Student's t test for 1 μM SR2 vs. vehicle), suggesting that there may be some tonic CB2R activation of cAMP in these cells.

One potential explanation for the CB2 increase in cAMP would be coupling to G_s G proteins. G_s-coupling has been described for the nominally $G_{i/o}$-coupled CB1 receptor (Glass and Felder, 1997). We therefore revisited cAMP production after pretreatment with either pertussis toxin (PTX) or cholera toxin (CTX). PTX effectively blocks $G_{i/o}$ signaling via ADP ribosylation of the $alpha_{i/o}$ subunit (Katada and Ui, 1982). If CB2 action on cAMP

accumulation were $G_{i/o}$-dependent then it should be blocked by pretreatment with PTX. We found that it was not (Fig. 2D–E; significant effect of JWH133 on cAMP accumulation using 1 way ANOVA and Bonferroni post-hoc test. Figure 2D: [$F(4,7) = 88.7$, $p = 0.02$]; Figure 2E: [$F(4,7) = 11.4$, $p = 0.02$]). CTX by contrast ADP-ribosylates the $alpha_s$ subunit but with the result that it constitutively activates the G_s-dependent signaling (Cassel and Pfeuffer, 1978). If the CB2 effects are G_s-dependent then CTX-treatment should occlude CB2 elevation of cAMP. Interestingly we found that not only was there no increase in cAMP after JWH133 treatment but instead CTX-treatment unmasked a CB2-mediated reduction in cAMP that was blocked by co-treatment with SR2 (Fig. 2F; significant effect of JWH133 on cAMP accumulation using 1 way ANOVA and Bonferroni post-hoc test. Figure 2D: [$F(4,7) = 25.3$, $p = 0.046$]).

3.3 Corneal injury raises levels of acylethanolamines in bovine cornea.

If endocannabinoids play a chemotaxic role in migration, then it is reasonable to expect measurable changes in endocannabinoid levels. We tested for changes in levels of ~35 cannabinoid related lipids, free fatty acids and metabolites. As shown in Table 1, we found that there was little change in levels of any of these lipids excepting the N-acyl ethanolamines, all but one of which saw elevations one hour after injury (See Methods and Supplementary Table 1 for statistical details and values). This category includes arachidonoyl ethanolamine, an endogenous ligand for CB1 and CB2 receptors (Devane et al., 1992).

3.4 CB2R receptor activation does not alter bovine CEC proliferation

To explore whether CB2R receptors alter proliferation of bCECs, we tested several concentrations of CB2R agonist JWH133, all without effect. EGF (50ng/mL) in the same preparation induced the expected robust increase in proliferation (Fig. 3, % increase in proliferation for EGF (50ng/mL): 246 ± 7; *, $p<0.05$, 1 way ANOVA with Dunnett's post hoc test vs. control). In the presence of EGF, JWH133 (1μM) did not alter cellular proliferation (data not shown). Neither the combination of JWH133 (1μM) + SR2 (1μM), nor SR2 (1μM) alone altered cellular proliferation. We conclude that CB2R receptor activation with JWH133 does not induce CEC proliferation.

3.5 No evidence of CB2R expression in cornea under baseline conditions in reporter mouse; expression is increased in injured cornea

The ongoing difficulty in obtaining credible CB2R protein staining by antibodies is widely recognized in the cannabinoid field, despite 20 years of efforts (Atwood and Mackie, 2010). We tested several commercially available CB2R antibodies for protein expression in anterior eye using immunohistochemistry with CB2R KO controls (data not shown, also see (Cecyre et al., 2014)). However, in each case the staining appeared to be non-specific as it was identical to the staining seen in CB2R KO mouse tissue.

CB2R reporter mice represent an alternative approach to address this question. This mouse model is engineered so that eGFP is co-expressed with the CB2R receptor; thus cells actively expressing CB2R will contain eGFP (see methods; (Lopez et al., 2018, In Press)). To increase signal we used an anti-eGFP antibody.

We examined eGFP expression in uninjured cornea from the reporter mice and found that it is not present under baseline conditions (Fig. 4A). Upon injury, eGFP expression is increased in the cornea (Fig. 4C). eGFP expression appears to be somewhat more pronounced in superficial cells (e.g. Fig. 5A) but interestingly, we did not observe greater staining at the wound edge (Fig. 4C, 5A). All individual migrating cells in the wound site at 1 hour expressed CB2R reporter.

3.6 Corneal CB2R mRNA expression is increased after injury

Using quantitative PCR (qPCR) we measured mRNA expression for cannabinoid receptors in injured (3 hrs) vs. uninjured eyes. We found that CB2R receptor expression was significantly elevated in injured relative to uninjured eyes (Fig 6A, mRNA levels in injured eyes (fold-change vs. uninjured (± SEM): 1.34 ± 0.11, n=12, $t(22) = 2.80$, $p=0.01$ by unpaired t test). CB1R expression was unaltered by injury (Fig. 6B; mRNA levels in injured eyes (fold-change vs. uninjured (± SEM): 0.98 ± 0.04, n=12, $t(22) = 0.35$, $p=0.73$ by unpaired t test).

3.7 CB1R deletion results in delayed wound closure.

We tested the consequences of cannabinoid receptor deletion on the rate of wound closure in an *in vivo* murine model of corneal wound healing. We tested the rate of wound healing in CB1R and CB2R KO mice. In CB1R KO mice we confirmed that CB1R deletion slows the rate of corneal wound healing, though by ~3 hours, somewhat less than the 8 hrs reported by Yang et al. (Yang et al., 2013).

3.8 CB2R deletion delays wound closure in vivo

We tested whether CB2R deletion would alter the course of wound closure. We found that CB2R KOs see delayed wound closure relative to wild type animals (Fig. 7B). Treatment with CB2R antagonist SR144528 (3mM) yielded a similar delay (Fig. 7C) as did treatment with the CB2R agonist JWH133 (3mM, Fig. 7D). We did not observe a sex-dependence of the delay in wound healing in either the CB1R or CB2R KOs (Supplemental Figure 2).

4 DISCUSSION

Our chief findings are 1) a CB2R signaling system is upregulated by injury in murine cornea; 2) CB1R deletion in mouse slows healing, consistent with a published finding; 3) CB2R deletion in mouse also slows wound closure; 4) in experiments using a different species, the cow, we find that levels of N-acyl ethanolamines including the eCB anandamide are increased upon injury in bovine cornea; 5) in epithelial cells cultured from cow eyes we find that CB2R activation mediates repulsive chemotaxis.

Corneal wound healing is highly choreographed, involving the directional migration of multiple cell types, some toward, some away, from the site of injury. It is likely that the movement of many of these cells is directed by chemotaxic cues. However, little is known about chemotaxic regulation of migration in the corneal epithelium. Yang et al. showed that CB1R deletion slows corneal wound healing in mice (Yang et al., 2013). This finding, taken together with our evidence that CB1R mediates chemotaxis in CECs offers a potential

mechanism for cannabinoid regulation of corneal wound healing, whereby endocannabinoids serve as lipid cues to direct migration of epithelial cells during the highly choreographed healing process. We revisited the course of wound healing in CB1R KO mice and confirmed the findings of Yang et al. that wound healing is slowed. The somewhat more rapid time course of closure seen in our experiments is likely due to the smaller wounds used in our preparation.

If migration of CECs is guided by a gradient of eCBs then one would expect altered levels of eCBs upon injury. Our finding in bovine cornea that injury elevates nearly all N-acyl ethanolamines tested including the CB1/CB2 endogenous ligand anandamide implicates these lipids as chemotaxic messengers.

Turning to CB2R, previous studies of mRNA expression in anterior eye (e.g. (Porcella et al., 1998; Porcella et al., 2000)) and our own experiments conducted in collaboration with Dr. Shu-Jung Hu, suggested that CB2R mRNA was not present under baseline conditions. However, using quantitative PCR and a recently developed CB2R reporter mouse we observed an upregulation of CB2R three hours after injury. Our immunohistochemical and mRNA expression data are therefore consistent with a CB2R role in corneal wound healing.

Functionally, we see evidence that CB2R mediates chemorepulsion in cultured corneal epithelial cells. Our *in vivo* data shows a delay in the net course of wound healing both from CB2R deletion and topical treatment with CB2R antagonists. The pharmacological blockade indicates that the difference is not due to an adaptive developmental effect in the CB2R KO. Topical treatment with a CB2 agonist also slowed wound healing, a result that may seem counterintuitive at first. However if we assume that some key migratory events are mediated by a gradient of CB2 receptor ligands, then a bath application of a CB2 ligand would in fact eliminate the gradient (since the concentration would be the same throughout the tissue).

We have previously reported that CB1 mediates chemoattraction of CECs and that CB1 activation reduces both cAMP levels and MAPK activity (Murataeva et al., 2015). In contrast CB2 activation induces chemorepulsion, elevation of cAMP levels and activation of MAPK. This arrangement is summarized schematically in Figure 8. Our experiments with pertussis toxin (PTX) and cholera toxin (CTX), which impact $G_{i/o}$ and G_s signaling respectively, suggest that CB2 receptors predominantly signal via G_s since cholera toxin, which constitutively activates G_s signaling, occluded the increase in cAMP that we saw with CB2 agonist treatment. However it is notable that CTX treatment appeared to unmask an CB2-mediated lowering of cAMP. It is possible therefore that CB2 acts both via $G_{i/o}$ and G_s in opposing directions but that G_s is dominant. In any event, it seems likely that the differential chemotaxic effects of these receptors are mediated by either altered cAMP, MAPK signaling, or both.

Epithelial cell proliferation occurs at a later stage in the process of corneal wound healing, as the corneal epithelial cells replenish their accustomed numbers. Yang et al (2013) reported that CB1R mediates an increase in CEC proliferation, a result that we were unable to replicate in bovine CECs (Murataeva et al., 2015). We also do not see a CB2R-mediated alteration of epithelial cell proliferation.

One significant unresolved question has to do with the identity and source of the endocannabinoid signal. Which endocannabinoid serves as the guidance cue and what cells produce that endocannabinoid? The two canonical endocannabinoids are 2-arachidonoyl glycerol (2-AG) (Sugiura et al., 1995) and arachidonoyl ethanolamide (AEA, anandamide) (Devane et al., 1992), two structurally related lipids. Yang et al. measured levels of 2-AG and AEA in uninjured WT mouse corneas, detecting only 2-AG (Yang et al., 2013), thus arguing for a 2-AG role. However we find that with injury in cow eyes there is a clear and specific increase in the levels of acyl-ethanolamines, including AEA, while levels of other cannabinoid-related lipids including 2-AG remain unaltered. Moreover, we have tested mouse corneas for expression of cannabinoid-related lipids and do detect AEA (data not shown), suggesting that the difference is due to differential detection limits (since AEA levels are often an order of magnitude lower than 2-AG (Cravatt et al., 2001)) rather than a species difference. Endocannabinoids are lipids that are produced ‘on demand’ enzymatically (Murataeva et al., 2013), so it is not surprising that levels of these should rise as a group. Synthesis of acyl-ethanolamines likely occurs via activity of NAPE-PLD (Leishman et al., 2016), message for which we have previously detected in bovine cornea (Murataeva et al., 2015). We have also shown that NAPE-PLD knockout mice see diminished levels of AEA in mouse eye (Miller et al., 2016). Our results therefore support a role for AEA over 2-AG in wound healing, and moreover suggest that the synthesis of acyl-ethanolamines occurs locally within the cornea rather than deriving from extraocular sources such as the lacrimal glands. However it should be stressed that there may be significant species differences in cannabinoid regulation of corneal function between the mouse and cow, not least due to the considerable difference in size.

To our knowledge this is the first evidence for a signaling system that underlies chemorepulsion in corneal epithelial cells. Though CB2R appears to be intimately involved in both wound healing and migration, additional work will be required to formulate a coherent model of a CB2R role in regulation of wound healing. In particular it will be essential to determine the circuitry of cannabinoid signaling. Which cannabinoids are produced under what circumstances by which cells. Our results from post-mortem injured cornea implicate local production of acyl-ethanolamines in early stage wound healing but this does not rule out additional contributions from extra-ocular sources such as the lacrimal glands or from the immune cells that migrate to the site of injury.

It may seem odd at first two related receptors should have opposing actions, perhaps even in the same cells. It is possible, however, that the balance of push/pull signals allows for a more fine-tuned migratory cue. Cells would migrate until they reach a point where the push/pull ratio is in balance, and loiter there, rather than simply migrating toward or away from the source.

Given the immune component in corneal healing, it may not be a coincidence that CB2R plays this role since CB2R is a receptor long associated with immune responses (Atwood and Mackie, 2010). Neutrophils responding to bacterial ingress outside the wound or leukocytes accumulating under the basement membrane may themselves respond to such cues (reviewed in (Cabral et al., 2015)) or might produce a repulsive cue, thereby allowing a flexible response to bacterial load in the site of injury.

One major question is to what extent these findings may be generalizable to other species and tissues. It is tempting to speculate that chemotaxic regulation of cell migration may be involved in wound healing in related tissues such as skin, but the cornea has unusual properties that may limit generalizability of our findings. In contrast to skin, the cornea is avascular and experiences major differences in terms of blood intrusion, coagulation, inflammation, scarring, and the overall timing of wound healing. It is therefore possible but not certain that this cannabinoid receptor-dependent signaling system is employed in other epithelial tissues that undergo responses to injury such as skin and the lining of the gut. Nearly all cells migrate at some point in their existence and so it is possible that cannabinoid-based migration cues will be found to play roles in other tissues. CB1 receptors are widely distributed in the brain and body (Buckley et al., 1998; Herkenham et al., 1990). However since the CB2 role described here required pathology-induced upregulation, any CB2 role in other tissues may also be restricted to pathological and/or immune-related conditions. There are tissues such as bone that express both receptors without the requirement for pathology; but taking the example of bone (Zimmer, 2016) CB1 and CB2 already have defined roles in bone remodeling. The implications of our in vivo experiments in mice, which have considerable size and structural differences in their cornea relative to other species such as humans, may also be limited, particularly when one considers that there are significant differences in wound healing even across mouse strains (Pal-Ghosh et al., 2008).

In summary, we find that cannabinoid CB2R receptors are upregulated upon injury in the mouse and that deletion of either cannabinoid CB1R or CB2R receptors impairs the normal course of healing. Moreover, we find that these receptors mediate chemorepulsion in cultured bovine corneal epithelial cells and that endocannabinoids levels rise with injury in bovine corneal explants. Our results indicate that CB2R receptors are involved in the normal course of healing, perhaps via regulation of chemotaxis.

Supplementary Material

Refer to Web version on PubMed Central for supplementary material.

Acknowledgements:

This work was supported in part by a grant from the National Institutes of Health [RO1-EY24625, AS].

Abbreviations:

ABHD12	a/b hydrolase domain containing 12
bCECs	bovinecorneal epithelial cells
CB1	cannabinoid receptor 1
CB2	cannabinoid receptor 2
GFP	green fluorescent protein
DMSO	dimethylsulfoxide

FRET	fluorescence resonance energy transfer

LITERATURE CITED

Atwood BK, Mackie K, 2010 CB2: a cannabinoid receptor with an identity crisis. Br J Pharmacol 160, 467–479. [PubMed: 20590558]

Bradshaw HB, Rimmerman N, Hu SS, Burstein S, Walker JM, 2009 Novel endogenous N-acyl glycines identification and characterization. Vitam Horm 81, 191–205. [PubMed: 19647113]

Buckley NE, Hansson S, Harta G, Mezey E, 1998 Expression of the CB1 and CB2 receptor messenger RNAs during embryonic development in the rat. Neuroscience 82, 1131–1149. [PubMed: 9466436]

Cabral GA, Ferreira GA, Jamerson MJ, 2015 Endocannabinoids and the Immune System in Health and Disease. Handb Exp Pharmacol 231, 185–211. [PubMed: 26408161]

Cairns EA, Toguri JT, Porter RF, Szczesniak AM, Kelly ME, 2015 Seeing over the horizon - targeting the endocannabinoid system for the treatment of ocular disease. J Basic Clin Physiol Pharmacol.

Cassel D, Pfeuffer T, 1978 Mechanism of cholera toxin action: covalent modification of the guanyl nucleotide-binding protein of the adenylate cyclase system. Proc Natl Acad Sci U S A 75, 2669–2673. [PubMed: 208069]

Cecyre B, Thomas S, Ptito M, Casanova C, Bouchard JF, 2014 Evaluation of the specificity of antibodies raised against cannabinoid receptor type 2 in the mouse retina. Naunyn Schmiedebergs Arch Pharmacol 387, 175–184. [PubMed: 24185999]

Cravatt BF, Demarest K, Patricelli MP, Bracey MH, Giang DK, Martin BR, Lichtman AH, 2001 Supersensitivity to anandamide and enhanced endogenous cannabinoid signaling in mice lacking fatty acid amide hydrolase. Proc Natl Acad Sci U S A 98, 9371–9376. [PubMed: 11470906]

Devane WA, Hanus L, Breuer A, Pertwee RG, Stevenson LA, Griffin G, Gibson D, Mandelbaum A, Etinger A, Mechoulam R, 1992 Isolation and structure of a brain constituent that binds to the cannabinoid receptor. Science 258, 1946–1949. [PubMed: 1470919]

Fiskerstrand T, H'Mida-Ben Brahim D, Johansson S, M'Zahem A, Haukanes BI, Drouot N, Zimmermann J, Cole AJ, Vedeler C, Bredrup C, Assoum M, Tazir M, Klockgether T, Hamri A, Steen VM, Boman H, Bindoff LA, Koenig M, Knappskog PM, 2010 Mutations in ABHD12 cause the neurodegenerative disease PHARC: An inborn error of endocannabinoid metabolism. Am J Hum Genet 87, 410–417. [PubMed: 20797687]

Gaoni Y, Mechoulam R, 1964 Isolation, structure and partial synthesis of an active constituent of hashish. J Am Chem Soc 86, 1646–1647.

Ghosh S, Preet A, Groopman JE, Ganju RK, 2006 Cannabinoid receptor CB2 modulates the CXCL12/CXCR4-mediated chemotaxis of T lymphocytes. Mol Immunol 43, 2169–2179. [PubMed: 16503355]

Glass M, Felder CC, 1997 Concurrent stimulation of cannabinoid CB1 and dopamine D2 receptors augments cAMP accumulation in striatal neurons: evidence for a Gs linkage to the CB1 receptor. J Neurosci 17, 5327–5333. [PubMed: 9204917]

He F, Song ZH, 2007 Molecular and cellular changes induced by the activation of CB2 cannabinoid receptors in trabecular meshwork cells. Mol Vis 13, 1348–1356. [PubMed: 17679938]

Herkenham M, Lynn AB, Little MD, Johnson MR, Melvin LS, de Costa BR, Rice KC, 1990 Cannabinoid receptor localization in brain. Proc Natl Acad Sci U S A 87, 1932–1936. [PubMed: 2308954]

Howlett AC, Breivogel CS, Childers SR, Deadwyler SA, Hampson RE, Porrino LJ, 2004 Cannabinoid physiology and pharmacology: 30 years of progress. Neuropharmacology 47 Suppl 1, 345–358. [PubMed: 15464149]

Kano M, Ohno-Shosaku T, Hashimotodani Y, Uchigashima M, Watanabe M, 2009 Endocannabinoid-mediated control of synaptic transmission. Physiol Rev 89, 309–380. [PubMed: 19126760]

Katada T, Ui M, 1982 ADP ribosylation of the specific membrane protein of C6 cells by islet-activating protein associated with modification of adenylate cyclase activity. J Biol Chem 257, 7210–7216. [PubMed: 7200979]

Ledent C, Valverde O, Cossu G, Petitet F, Aubert JF, Beslot F, Bohme GA, Imperato A, Pedrazzini T, Roques BP, Vassart G, Fratta W, Parmentier M, 1999 Unresponsiveness to cannabinoids and reduced addictive effects of opiates in CB1 receptor knockout mice. Science 283, 401–404. [PubMed: 9888857]

Leishman E, Mackie K, Luquet S, Bradshaw HB, 2016 Lipidomics profile of a NAPE-PLD KO mouse provides evidence of a broader role of this enzyme in lipid metabolism in the brain. Biochim Biophys Acta 1861, 491–500. [PubMed: 26956082]

Li SS, Wang LL, Liu M, Jiang SK, Zhang M, Tian ZL, Wang M, Li JY, Zhao R, Guan DW, 2016 Cannabinoid CB(2) receptors are involved in the regulation of fibrogenesis during skin wound repair in mice. Mol Med Rep 13, 3441–3450. [PubMed: 26935001]

Lopez A, Aparicio N, Pazos MR, Grande MT, Barreda-Manso MA, Benito I, Vazquez C, Amores M, Ruiz-Perez G, Garcia-Garcia E, Beatka M, Tolon RM, Dittel BN, Hillard C, Romero J, 2018, In Press. Cannabinoid CB2 receptors in the mouse brain: Relevance for Alzheimer's disease. Journal of Neuroinflammation.

Lu Q, Straiker A, Maguire G, 2000 Expression of CB2 cannabinoid receptor mRNA in adult rat retina. Vis Neurosci 17, 91–95. [PubMed: 10750830]

Meijering E, Dzyubachyk O, Smal I, 2012 Methods for cell and particle tracking. Methods Enzymol 504, 183–200. [PubMed: 22264535]

Miller S, Hu SS, Leishman E, Morgan D, Wager-Miller J, Mackie K, Bradshaw HB, Straiker A, 2017 A GPR119 signaling system in the murine eye regulates intraocular pressure in a sex-dependent manner. Invest Ophthalmol Vis Sci 58, 2930–2938. [PubMed: 28593245]

Miller S, Leishman E, Oehler O, Daily L, Murataeva N, Wager-Miller J, Bradshaw H, Straiker A, 2016 Evidence for a GPR18 role in diurnal regulation of intraocular pressure. Invest Ophthalmol Vis Sci 57, 6419–6426. [PubMed: 27893106]

Munro S, Thomas KL, Abu-Shaar M, 1993 Molecular characterization of a peripheral receptor for cannabinoids. Nature 365, 61–65. [PubMed: 7689702]

Murataeva N, Dhopeshwarkar A, Yin D, Mitjavila J, Bradshaw H, Straiker A, Mackie K, 2016 Where's my entourage? The curious case of 2-oleoylglycerol, 2-linolenoylglycerol, and 2-palmitoylglycerol.Pharmacol Res 110, 173–180. [PubMed: 27117667]

Murataeva N, Li S, Oehler O, Miller S, Dhopeshwarkar A, Hu SS, Bonanno JA, Bradshaw H, Mackie K, McHugh D, Straiker A, 2015 Cannabinoid-induced chemotaxis in bovine corneal epithelial cells. Invest Ophthalmol Vis Sci 56, 3304–3313. [PubMed: 26024113]

Murataeva N, Mackie K, Straiker A, 2012 The CB2-preferring agonist JWH015 also potently and efficaciously activates CB1 in autaptic hippocampal neurons. Pharmacol Res 66, 437–442. [PubMed: 22921769]

Murataeva N, Straiker A, Mackie K, 2013 Parsing the players: 2-AG synthesis and degradation in the CNS. Br J Pharmacol 171, 1379–1391.

Pal-Ghosh S, Tadvalkar G, Jurjus RA, Zieske JD, Stepp MA, 2008 BALB/c and C57BL6 mouse strains vary in their ability to heal corneal epithelial debridement wounds. Exp Eye Res 87, 478–486. [PubMed: 18809399]

Porcella A, Casellas P, Gessa GL, Pani L, 1998 Cannabinoid receptor CB1 mRNA is highly expressed in the rat ciliary body: implications for the antiglaucoma properties of marihuana. Brain Res Mol Brain Res 58, 240–245. [PubMed: 9685662]

Porcella A, Maxia C, Gessa GL, Pani L, 2000 The human eye expresses high levels of CB1 cannabinoid receptor mRNA and protein. Eur J Neurosci 12, 1123–1127. [PubMed: 10762343]

Straiker A, Stella N, Piomelli D, Mackie K, Karten HJ, Maguire G, 1999a Cannabinoid CB1 receptors and ligands in vertebrate retina: localization and function of an endogenous signaling system. Proc Natl Acad Sci U S A 96, 14565–14570. [PubMed: 10588745]

Straiker AJ, Maguire G, Mackie K, Lindsey J, 1999b Localization of cannabinoid CB1 receptors in the human anterior eye and retina. Invest Ophthalmol Vis Sci 40, 2442–2448. [PubMed: 10476817]

Sugiura T, Kondo S, Sukagawa A, Nakane S, Shinoda A, Itoh K, Yamashita A, Waku K, 1995 2-Arachidonoylglycerol: a possible endogenous cannabinoid receptor ligand in brain. Biochem Biophys Res Commun 215, 89–97. [PubMed: 7575630]

Wang LL, Zhao R, Li JY, Li SS, Liu M, Wang M, Zhang MZ, Dong WW, Jiang SK, Zhang M, Tian ZL, Liu CS, Guan DW, 2016 Pharmacological activation of cannabinoid 2 receptor attenuates inflammation, fibrogenesis, and promotes re-epithelialization during skin wound healing. Eur J Pharmacol 786, 128–136. [PubMed: 27268717]

Wright K, Rooney N, Feeney M, Tate J, Robertson D, Welham M, Ward S, 2005 Differential expression of cannabinoid receptors in the human colon: cannabinoids promote epithelial wound healing. Gastroenterology 129, 437–453. [PubMed: 16083701]

Yang Y, Yang H, Wang Z, Varadaraj K, Kumari SS, Mergler S, Okada Y, Saika S, Kingsley PJ, Marnett LJ, Reinach PS, 2013 Cannabinoid receptor 1 suppresses transient receptor potential vanilloid 1-induced inflammatory responses to corneal injury. Cell Signal 25, 501–511. [PubMed: 23142606]

Zheng JL, Yu TS, Li XN, Fan YY, Ma WX, Du Y, Zhao R, Guan DW, 2012 Cannabinoid receptor type 2 is time-dependently expressed during skin wound healing in mice. Int J Legal Med 126, 807–814. [PubMed: 22814434]

Zhong L, Geng L, Njie Y, Feng W, Song ZH, 2005 CB2 cannabinoid receptors in trabecular meshwork cells mediate JWH015-induced enhancement of aqueous humor outflow facility. Invest Ophthalmol Vis Sci 46, 1988–1992. [PubMed: 15914613]

Zimmer A, 2016 A collaboration investigating endocannabinoid signalling in brain and bone. J Basic Clin Physiol Pharmacol 27, 229–235. [PubMed: 26887036]

Highlights:

- Functional cannabinoid CB2 receptors are upregulated upon injury in corneal epithelium
- CB2 receptor deletion impairs the course of wound healing.
- CB2 receptors mediate chemorepulsion in corneal epithelial cells.
- CB2 receptors do not alter the epithelial cell proliferation.
- Findings suggest that like CB1, cannabinoid CB2 receptors play a role in the course of wound healing, but via chemorepulsion.

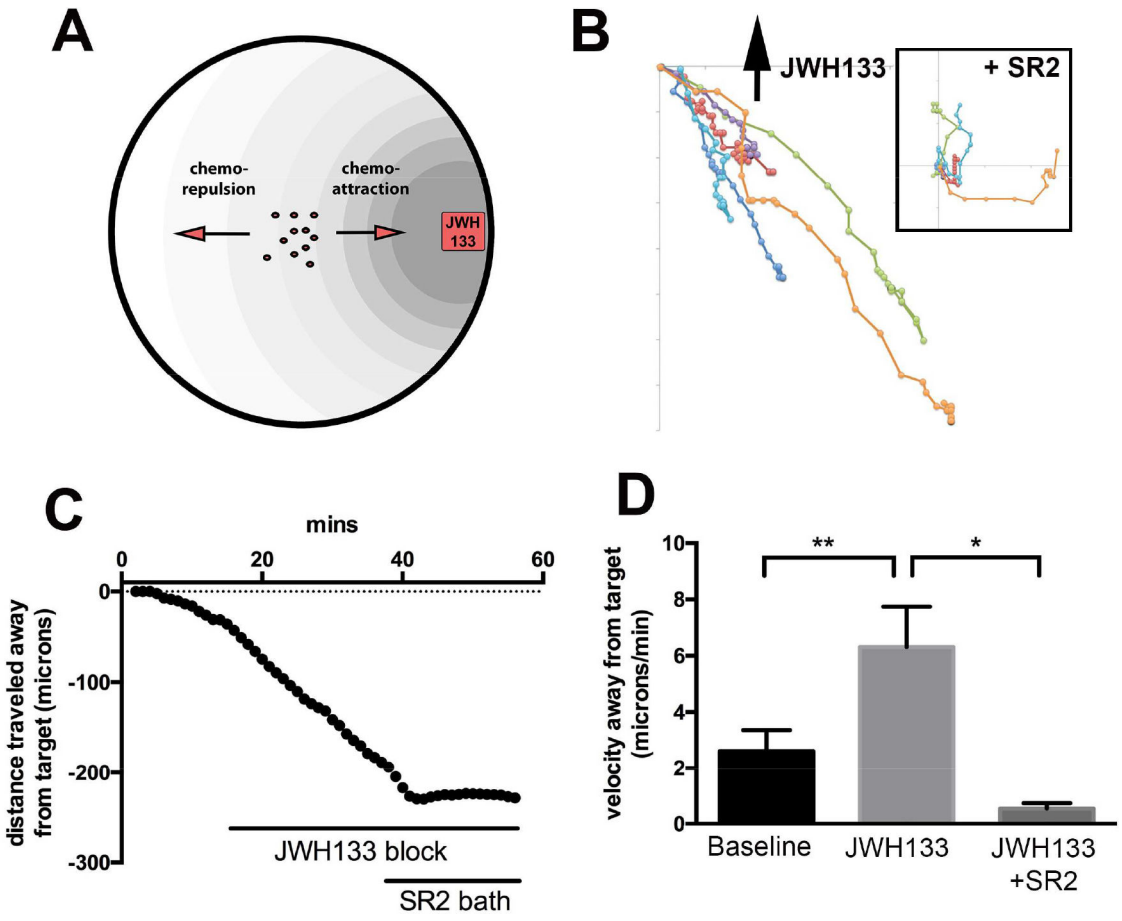

Figure 1. CB2R activation mediates chemorepulsion in bovine corneal epithelial cells.

A) Schematic illustrating in-dish migration assay with drug- embedded agar block. B) Cell tracking from representative experiment. Direction of agar block indicated by arrow. Inset shows subsequent migration of same cells after bath application of SR2, with starting points normalized to the origin to facilitate comparison. C) Net distance traveled relative to agar cube containing JWH133 (300nM), before and after bath application of CB2R antagonist SR144528 (SR2, 250nM). D) Bar graph summarizes velocities away from target. *, $p<0.05$, **, $p<0.01$, One-way ANOVA with Bonferroni post hoc test.

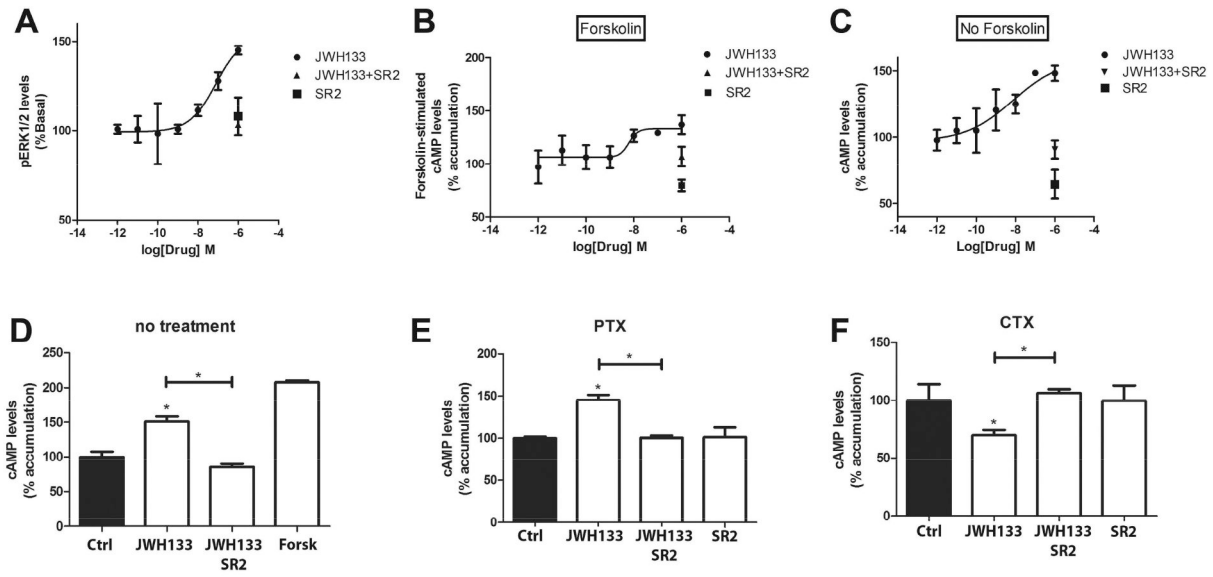

Figure 2. CB2R activation increases MAPK signaling and activates adenylyl cyclase in bovine CECs.

A) phosphoERK (pERK) levels are increased in a concentration-dependent manner by CB2R agonist JWH133. This effect is blocked by CB2R antagonist SR144528 (SR2, 1μM, $p<0.001$, Student's t test for 1μM concentrations). B) JWH133 modestly increases adenylyl cyclase activity even in the presence of adenylyl cyclase activator forskolin. C) In the absence of forskolin, JWH133 induces an increase in cAMP. SR2 (1μM) alone substantially lowers cAMP accumulation, indicating tonic activity or off target effects. D-F) cAMP accumulation was revisited with pertussis toxin (PTX) or cholera toxin (CTX) pretreatment. D) Control shows increase with 1uM JWH133 as expected from prior results. E) Same experiment after PTX pretreatment shows that effect is maintained. F) CTX pretreatment however unmasked a suppression of cAMP production. *, $p<0.05$, 1 way ANOVA with Bonferroni post hoc test.

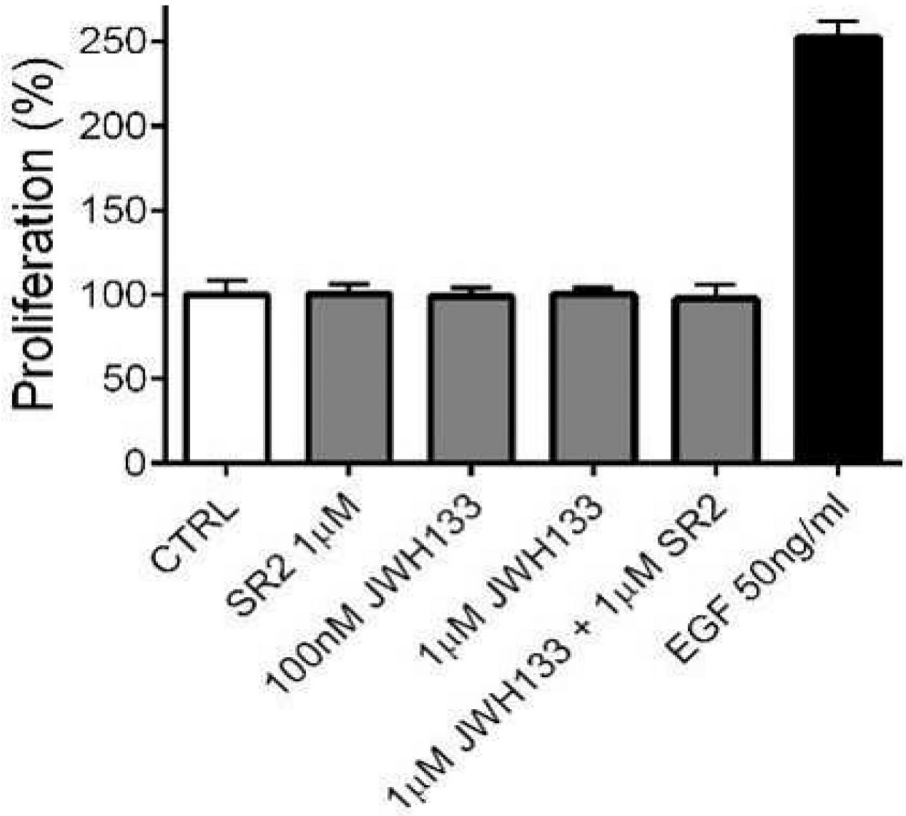

Fig. 3: JWH133 does not enhance proliferation of bCECs.

In a proliferation assay, JWH133 (100nM and 1 μM) and SR2 (1 μM) do not alter bCEC proliferation. 14 $P>0.05$, 1 way ANOVA with Bonferroni post hoc vs. control. EGF increases proliferation significantly $p<0.05$ 1 way ANOVA with Dunnett's post hoc vs. control.

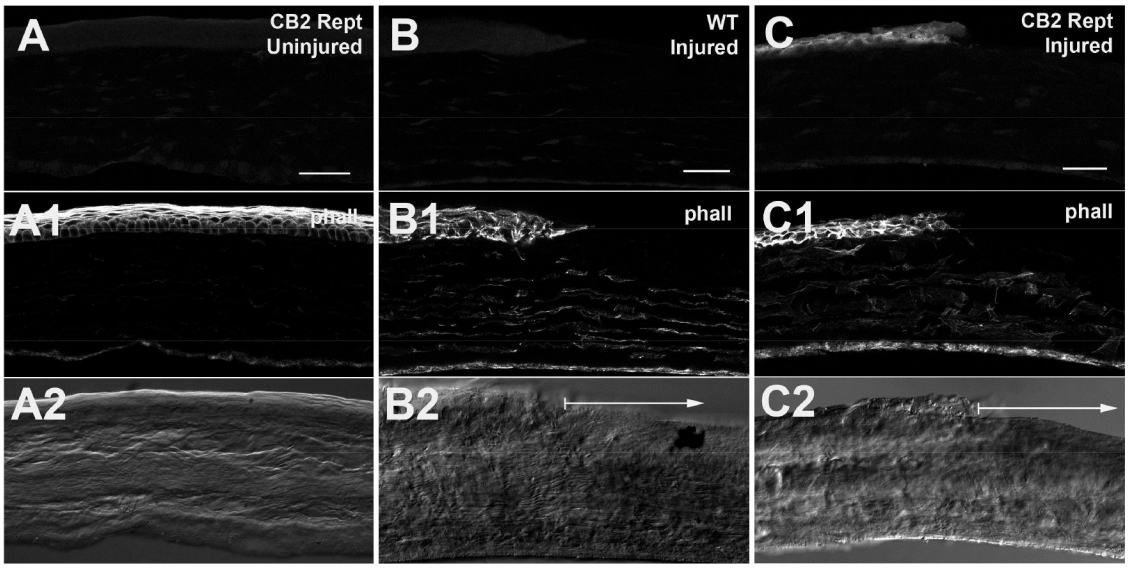

Figure 4. eGFP expression in cornea of reporter mice.

A) eGFP expression in uninjured corneas of CB2R reporter mice stained with anti-GFP antibody. A1) phalloidin staining outlines epithelial cells. A2) Corresponding DIC image. B) Injured WT control staining same anti-GFP antibody. B1, B2 as in A. Arrow in B2 shows region of wound. C) GFP staining in injured CB2R reporter cornea. C1, C2 as in A. Arrow in C2 shows region of wound. Scale bars: A) 35μm; B-C) 40μm.

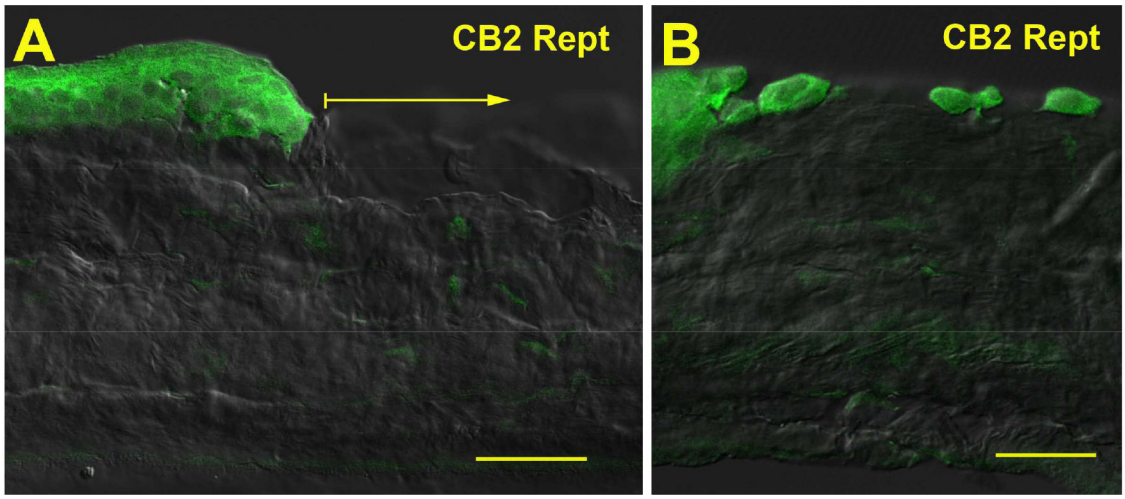

Figure 5. eGFP immunoreactivity in epithelial cells of injured cornea.

A) CB2R reporter expression in cells at wound edge at 1 hour post-injury. Arrow shows wound area. B) CB2R reporter expression in individual cells that have migrated into the wound site. Scale bars: A) 30 μm; B) 25 μm.

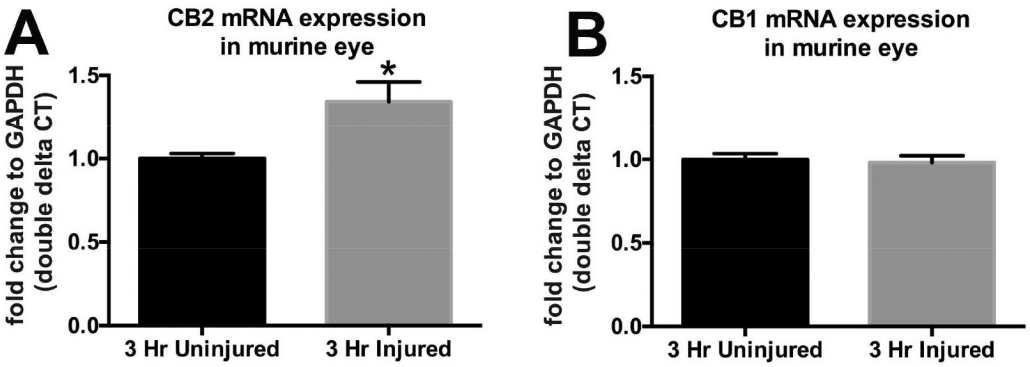

Figure 6. CB2R mRNA expression is upregulated in mouse eye after corneal injury.

Using quantitative PCR (qPCR) we tested mRNA expression for cannabinoid receptors in injured (3 hrs) vs. uninjured enucleated eyes. A) CB2R receptor expression was elevated in injured relative to uninjured eyes. B) CB_1 expression was unaltered by injury.*, $p<0.05$ by unpaired t-test.

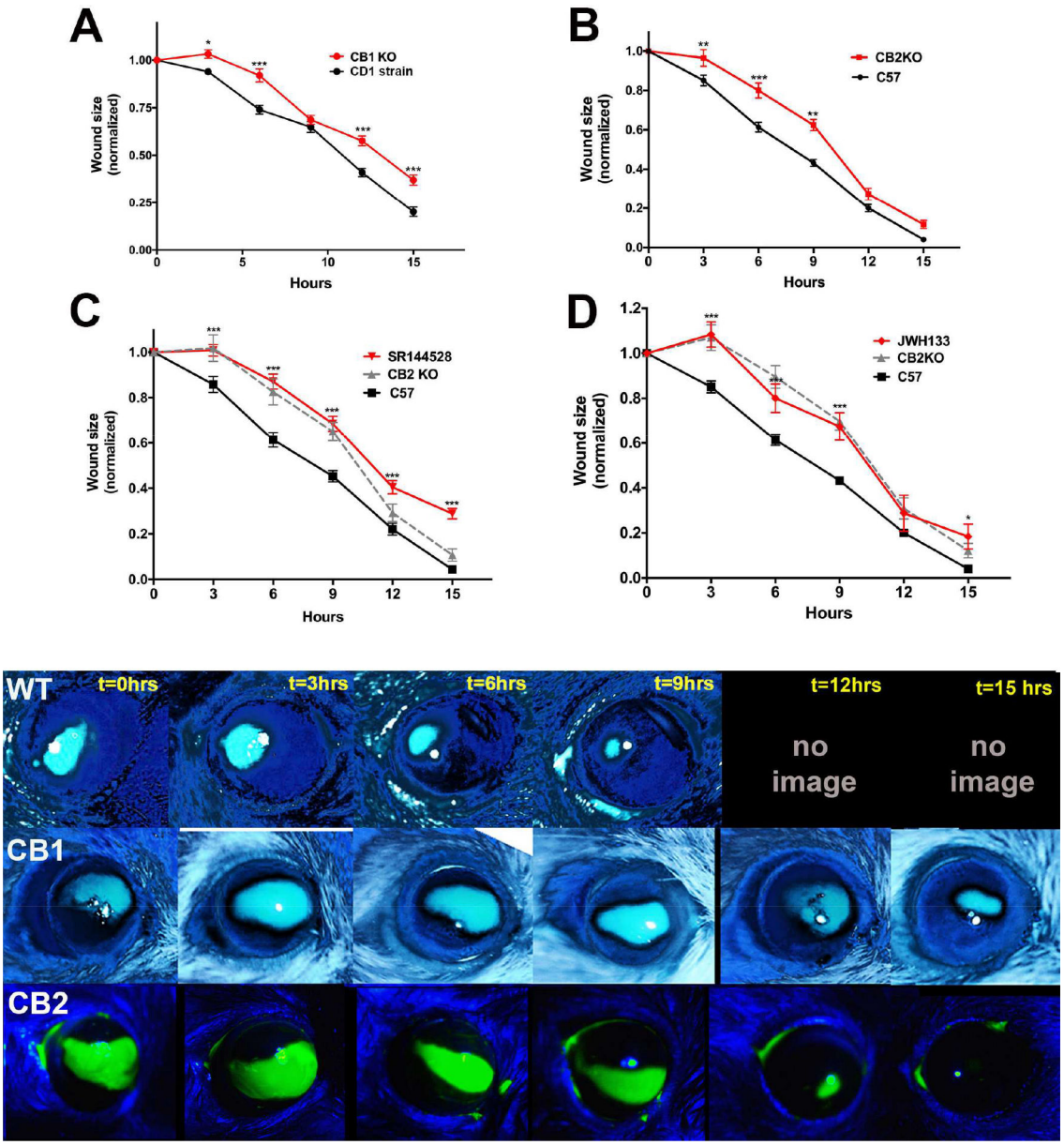

Figure 7. Deletion of CB_1 and CB2R cannabinoid receptors differentially alters the rate of wound healing in mice.

A) WT mice heal fully by 12–15 hours. CB1R KOs see delayed wound closure relative to CD1 strain controls. B) CB2R KOs also see delayed wound closure relative to C57Bl/6 (C57) strain controls. C) Treatment with CB2R antagonist SR144528 (3mM) mimics the delay in healing. D) CB2R agonist JWH133 also results in a similar time course to that for CB2R KOs. Lower panel: Sample time courses from WT, CB1R KO and CB2R KO eyes. *, $p<0.05$, **, $p<0.01$, ***, $p<0.001$, 2-way ANOVA with Bonferroni post hoc test.

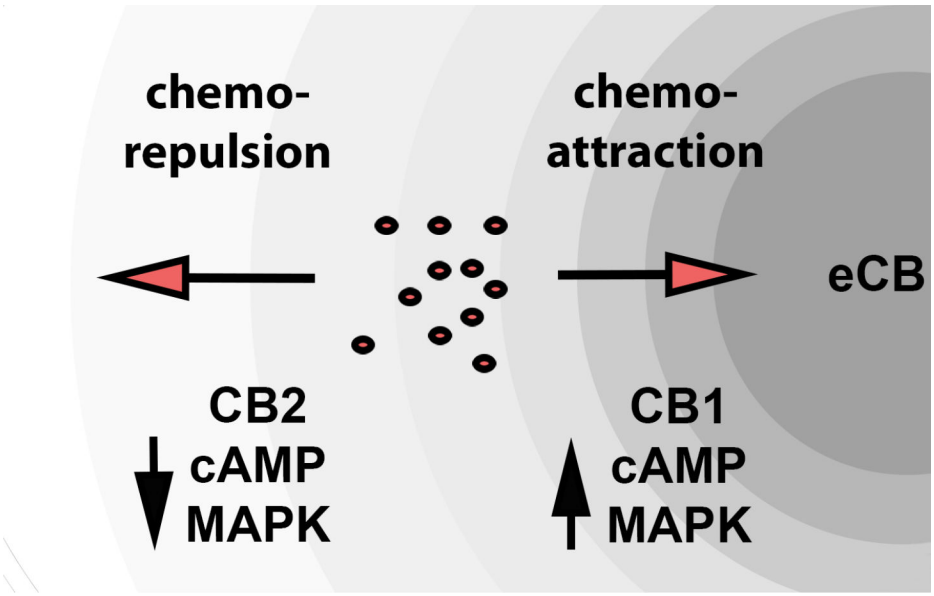

Figure 8. Schematic of opposing CB1 and CB2 regulation of epithelial cell chemotaxis.
Diagram depicts contrasting cAMP and MAPK signaling of CB1 and CB2 receptor as well as their opposing effects on chemotaxis.

Table 1.

Lipidomic analysis of endocannabinoids after 1 hour injury in bovine cornea.

1 arrow: 1–1.49x higher than control. 3 arrows: 2–2.99x higher then control. Light green: trending change. Green: statistically significant.

	Change with injury
***N*-acyl alanine**	
N-palmitoyl alanine	
N-stearoyl alanine	↑
N-oleoyl alanine	
N-llnoleoyl alanine	
N-arachidonoyl alanine	
N-docosahexaenoyl alanine	
***N*-acyl ethanolamine**	
N-palmitoyl ethanolamine	↑↑↑
N-stearoyl ethanolamine	↑↑↑
N-oleoyl ethanolamine	↑↑↑
N-linoleoyl ethanolamine	↑↑↑
N-arachidonoyl ethanolamine	↑↑↑
N-docosahexaenoyl ethanolamine	
***N*-acyl glycine**	
N-palmitoyl glycine	
N-stearoyl glycine	
N-oleoyl glycine	
N-linoleoyl glycine	
N-arachidonoyl glycine	
N-docosahexaenoyl glycine	
***N*-acyl leucine**	
N-palmitoyl leucine	
N-stearoyl leucine	
N-oleoyl leucine	
N-linoleoyl leucine	
N-docosahexaenoyl leucine	
***N*-acyl serine**	
N-palmitoyl serine	
N-stearoyl serine	
N-oleoyl serine	
N-linoleoyl serine	
N-arachidonoyl serine	
N-docosahexaenoyl serine	
***N*-acyl taurine**	

	Change with injury
N-arachidonoyl taurine	
Free Fatty Acids	
Linoleic acid	
Arachidonic acid	
2-acyl-*sn*-glycerol	
2-arachidonoyl-*sn*-glycerol	
2-linoleoyl-*sn*-glycerol	
2-oleoyl-*sn*-glycerol	
Prostaglandins	
PGE_2	